

A Design of New Surface Gradient Coil and Its Application to MR Computerized Tomography

Jeonghan Yi* and Zanghee Cho**

= Abstract =

A new three-channel surface gradient coil obtained by using numerical optimization and its application to MR computerized tomography are presented. The new surface gradient coil provided linear field gradient region more than twice wider compared with the first surface gradient coil, removed torque and field offset, and reduced coupling between the surface gradient coil and combined surface rf coil. We realized the new surface gradient coil set with $30 \times 60 \text{cm}^2$ size, which generated more than 4G/cm with 100 amperes over a $4 \times 4 \times 4 \text{cm}^3$ region with good linearity. The optimal geometries of the three-channel surface gradient coil and volunteer's high-resolution *in vivo* spinal cord images obtained by using the optimized surface gradient coil set are presented.

1. INTRODUCTION

From the invention of magnetic resonance (MR) imaging, there have been great needs in *in vivo* high-resolution human imaging in clinical applications even though only a few results of the *in vivo* high-resolution human imaging have been reported mainly due to the difficulties in the preparation of proper hardwares[1-4]. The most important instrumentation problem in the high-resolution imaging appears to be the need to increase the magnetic field gradients in order to achieve greater spatial resolution by greater frequency dispersion. Strong field gradient is usually obtained by reducing conventional coil structures, (e. g., the combination of G_x and G_y and Helmholtz coil for G_z),

and many results performed with the miniaturized gradient coils were presented[5]. The reduction of the conventional gradient coil size is inapplicable to the high-resolution *in vivo* human imaging in which strong gradients as well as large accessible area are essential. To overcome the problems, we have presented a three-channel surface gradient coil(SGC), which was constructed on a flat surface and high-resolution *in vivo* human images obtained by using these surface gradient coil[6, 7]. The surface gradient coil we have developed provided strong three orthogonal field gradients at near-SGC regions with the conventional gradient coil driver, fairly good linearity at the image centre, and furthermore, eddy current free field gradients since the SGC is always far from the conductive inner wall of main magnet. BY comparing the SGC with the conventional gradient coil, the flat structure of the SGC promises not only applicability to large objects without the

〈접수 : 1992년 8월 28일〉

* Dept. of Electrical Engineering, KAIST.

** Dept. of Information and Communication Engineering, KAIST.

object size problem but also easy combination with a surface rf coil. The loss of signal-to-noise ratio(SNR) in the high-resolution imaging is partly compensated by the adoption of smaller rf coil such as the surface rf coil[8]. This has the additional advantage of decreased field-of-view(FOV), i. e. a localization. The disadvantage of the smaller FOV is that the interiors of large objects become inaccessible. However, the smaller surface rf coil still provides sensitivity gains when a region-of-interest(ROI) is the exterior of an object, and combined SGC provides strong field gradients, which satisfy the requirements of *in vivo* high-resolution human imaging, especially for the exterior region of human body. The surface gradient coil can be applied for any imaging sequences, and would be suitable to the experiments that require strong gradients and/or fast gradient switching without the complex modification of existing system.

While the first SGC we have presented provided the field gradients with good linearity on the parallel planes, rapidly decreasing gradients along the depth direction was a drawback, which was inevitable because of asymmetric (one-sided) structure. Thus the first SGC was more suitable for the imaging of the planes parallel to the SGC than the orthogonal planes or 3-D volume. The other problems of the first SGC are the generation of strong torque when large driving current flows on the G_z coil, and the strong field offset of G_y coil due to its one-sided structure with unidirectional currents. The torque obstructs the generation of strong field gradient or fast switching, and the field offset causes image shift or requires the large frequency shift of selective rf pulses. In this paper, therefore, the new geometry of the three-channel surface gradient coil obtained by using numerical optimization to solve the problems of

the first SGC is presented. The new SGC expands linear field gradient region along the depth direction and removes the other problems of the first SGC, namely the torque and the field offset.

2. DESIGN OF NEW SURFACE GRADIENT COIL

Numerous algorithms of numerical optimization have been developed and each algorithm has efficient application area. Selection of the optimization algorithm was referred to guidance [9-11] and the Rosenbrock method was chosen as the most suitable method for the problem of SGC optimization in which multiple variables to be optimized are included. While the optimization of the SGC with unlimited dimensions will provide ideal gradients with respect to the linearity itself, the wide expansion of the SGC structure will cause the rapid increase of inductance or the decrease of generated field gradient. There are, therefore, some physical restrictions on the design of the SGC mainly due to the size of magnet inner bore, strengths of the field gradients, and inductances of the windings. Another consideration is the requirement of structural simplicity since complex structure is not easy to realize correctly.

The goals of the optimization are to obtain ; maximized linearity with strong field gradients, minimized inductances to ensure fast switching, and minimized number of active line-elements with proper distribution over the plane for the convenience of construction. In addition, removing the field offset of the G_y coil and torque of the G_z coil are also important goals of the new design. The parameters involved for the optimization are positions and current distributions of active line-elements.

Objectives and constraints of the optimization are as follows : The first aim of the optimiza-

tion is to obtain volunteer’s high-resolution images of spinal cord with at least $200\mu\text{m}$ resolution. Maximum size of the SGC is $30\text{cm} \times 60\text{cm}$, that is decided from the size of the human body. Objective imaging region along the depth(y) is $3\text{cm} \sim 13\text{cm}$. We set the y_0 (the null-field position) = 7cm by referring to the position of the spinal cord of human. On the other hand, the y_0 of the first SGC is ∞ . Note here that 3cm space is prepared for constructing the SGC set. The ROI for the optimization is ; $-5\text{cm} \leq x \leq 5\text{cm}$, $3\text{cm} \leq y \leq 13\text{cm}$, and $-5\text{cm} \leq z \leq 5\text{cm}$. Actually, the optimization was performed over two orthogonal planes($x-z$ and $y-z$ planes) rather than the 3-D volume for fast calculation because fields of the 3-D volume can be expected from the fields of these two planes. The required gradient strength of $200\mu\text{m}$ resolution with 256×256 image array and 5.12ms data sampling is 2.3G/cm for ^1H . To satisfy the requirement and to insure the selection of thin slices, the objective gradient strength was 4G/cm by using a $100\text{amp}/200$ volt driver.

Final geometries and current distributions(i. e., the number of turns in the figures) obtained by the optimization procedure are shown in Figs. 1(a)-(c) and field patterns are shown in Figs. 2(a)-(d). In figure 1(c), broken lines are used for cancelling the torque generated by the interaction between the currents on the active line-elements and strong main magnetic field by satisfying $N_1z_1 + N_2z_2 = N_2z_3$. In figure 2, the lines represent equifield contours and unshaded regions represent linear field gradient regions with $\pm 10\%$ error. The linear regions of the G_x and G_z coils are expanded more than twice wider by optimization. The G_y coil, on the contrary, provides narrow liner region even if optimized, which is a pay for the field offset correction. If one wants to obtain $G_y = 2.3\text{G/cm}$ for $200\mu\text{m}$ resolution, the field offset of the first

SGC at y_0 will be 36.8G and it will cause the frequency shift of 156.6kHz for ^1H . This shift is larger than the conventional image bandwidth, i. e., 20kHz , and can cause rf off-resonance problem, thereby reducing rf coil gain. It is also expected that images obtained with the large frequency shift will be ruined by system instabilities, e. g., drifts of rf generator, main magnetic field, and gradient system. However, G_y of

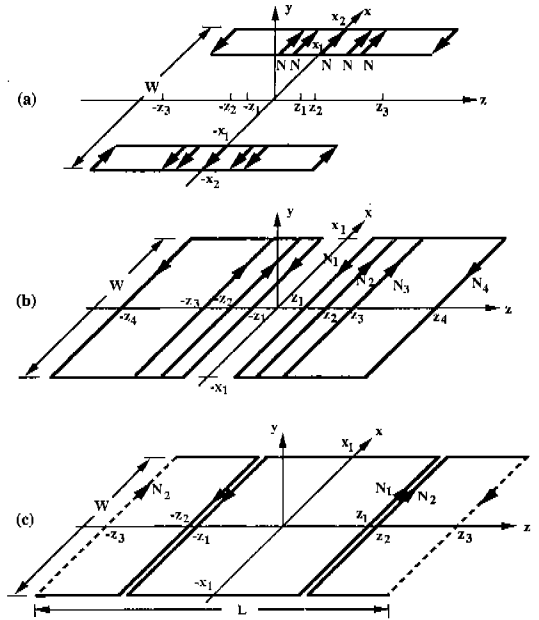


Fig. 1 Geometries of the new surface gradient coil. (a) is the G_x coil ($N=24$ turns, $x_1=10\text{cm}$, $x_2=15\text{cm}$, $z_1=3.5\text{cm}$, $z_2=5.0\text{cm}$, and $z_3=20\text{cm}$), (b) is the G_y coil ($N_1=17$ turns, $N_2=19$ turns, $N_3=30$ turns, $x_1=15\text{cm}$, $z_1=5.5\text{cm}$, $z_2=9.2\text{cm}$, $z_3=13.7\text{cm}$, and $z_4=25\text{cm}$), and (c) is the G_z coil ($N_1=N_2=25$ turns, $x_1=15\text{cm}$, $x_2=14.5\text{cm}$, $z_1=15.5\text{cm}$, and $z_2=30\text{cm}$). The three channels are constructed by overlapping on a plate so that forming a set of three-channel SGC. The broken lines of the G_z coil are used for cancelling the torque and the arrows depict directions of the current follow.

the first SGC will be more favorable if the field offset is allowable.

As discussed above, the optimized SGC has the geometries suitable for being combined with a surface rf coil since there are no line-elements at the central region of the new SGC, which means that there is negligible interaction between the new SGC and combined surface rf coil. This is an important merit of the SGC together with the generation of strong gradients

with conventional gradient driver. For the imaging of deeper or shallower region, the scales of the SGC can be enlarged or reduced to obtain better linearity and stronger or faster gradients according to circumstances. It is remarkable as shown in Fig. 1 that the active line-elements, except some return-paths, of the new SGC are placed at different z -positions so that thickness of constructed wires will be thinner than the first SGC.

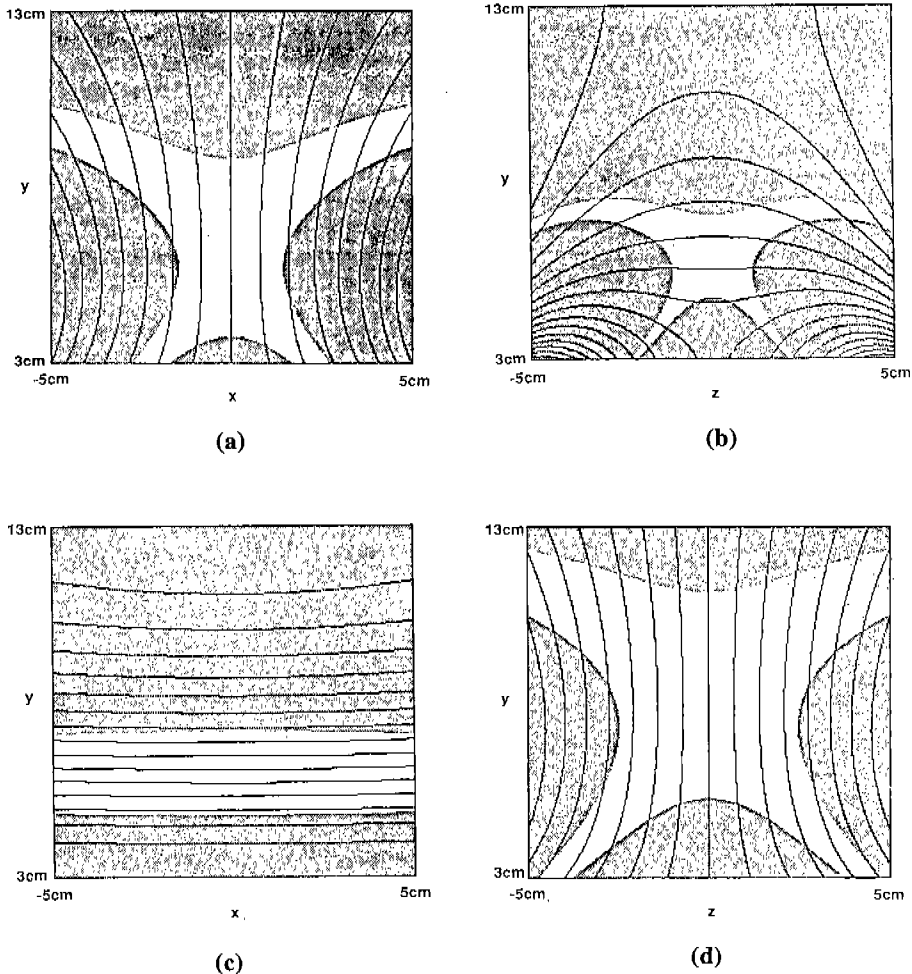


Fig. 2 Plots of 2-D magnetic field patterns with equifield contours : (a) is the G_x coil field of $z=0$ plane, (b) is the G_y coil field of $z=0$ plane, (c) is the G_y coil field of $x=0$ plane, and (d) is the G_z coil field of $x=0$ plane.

3. EXPERIMENTAL RESULTS

Figure 3 is an SGC realized on a $35 \times 70 \text{cm}^2$ acrylic plate with the optimal geometries shown in Fig. 1. A $12 \text{cm} \phi$ 2-turn surface rf coil is added at the centre of the SGC thereby forming a perfect surface imaging probe suitable for *in vivo* high-resolution imaging. By using the surface rf coil, better SNR than the body coil at the region of $0 \sim 10 \text{cm}$ depth is obtained. There is no Faraday shielding between the SGC and the surface rf coil because there are a little overlapping between the two coils. The maximum field gradients of 5G/cm (G_x and G_y) and 4G/cm (G_z) are obtained with 100amperes. These gradient strengths are surplus to $200 \mu\text{m}$ resolution imaging. Inductances and resistances are ; $2.6 \text{mH} + 1.6 \text{ohm}$ (G_x coil), $1.4 \text{mH} + 1.0 \text{ohm}$ (G_y coil), and $1.6 \text{mH} + 1.1 \text{ohm}$ (G_z coil) when each channel is wound by $0.7 \text{mm} \phi$ enamel coated copper wires. Epoxy resin is covered over the whole SGC plane for firm construction. The combined surface rf coil were used both for the transmission of excitation rf pulses and for the reception of NMR signals during all the experi-

ments. For the experimental verification of realized optimal SGC, we performed a set of linearity phantom imaging(Fig. 4) and high-resolution *in vivo* human imaging(Fig. 5). Figure 4(a) is a spin-echo image of a water-filled grid phantom obtained by conventional gradient coil and head coil. The phantom is constructed with 10×10 of $1 \times 1 \text{cm}^2$ acrylic bars with 2mm gaps and 4bars at the centre are replaced by 4×4 of $4 \times 4 \text{mm}^2$ bars. Figures 4(b) and (c), images of two orthogonal planes, are obtained by using the surface gradient coil set. These images present good linearity at the central region of the images, which manifest that the new SGC is suitable for high-resolution imaging of large object such as human body as desired. Figure 5 (a) is a conventional spin-echo image obtained with conventional gradient coil and the surface rf coil. Figures 5(b) is a high-resolution gradient-echo image obtained by using the SGC-surface rf coil set. The figure 5(b) is obtained by using conventional gradient-echo sequences with twice over-sampling along the phase-encoding direction without any localization method. Resolution of the high-resolution image is $200 \mu\text{m} \times 200 \mu\text{m} \times 3 \text{mm}$ and imaging time is

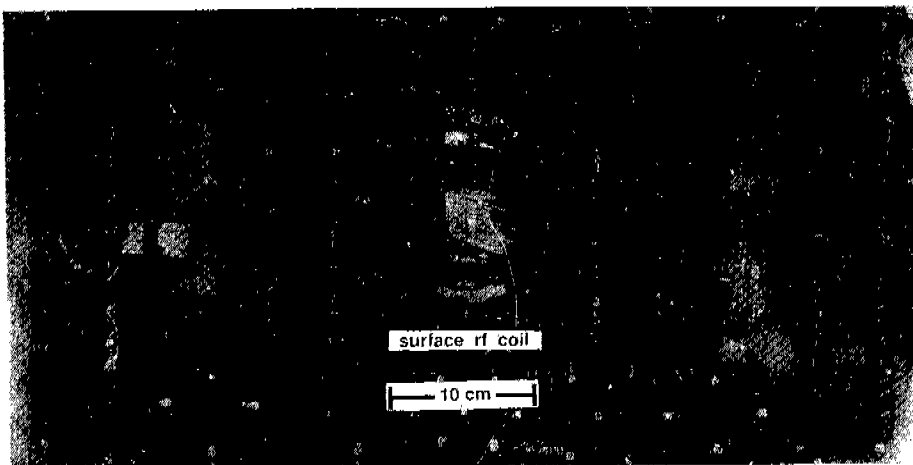


Fig. 3 The photo of the optimized surface gradient coil constructed on an acrylic plate.

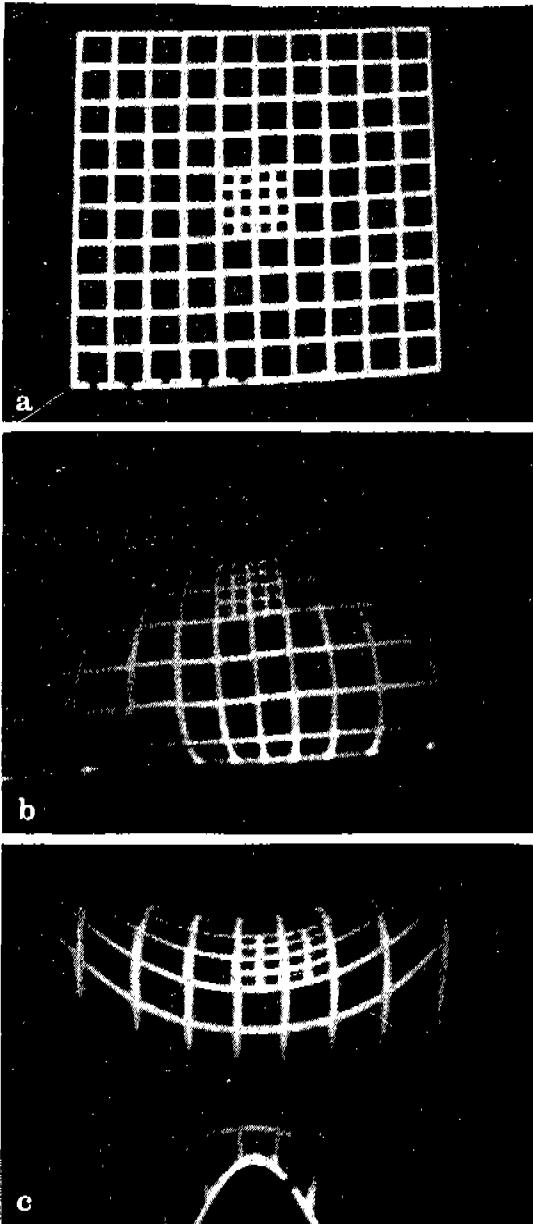


Fig. 4 Images of a water-filled phantom : (a) is the reference image of the water-filled phantom obtained by using conventional gradient coil and head coil and (b) and (c) are the images of $z=0$ and $x=0$ planes obtained by using the SGC+surface rf coil set to test the linearity.

30min. Figures 5(b) shows the more details of spinal cord than the results ever been reported.

4. CONCLUSIONS

We developed a new 3-channel SGC by using numerical optimization and proved its perfor-

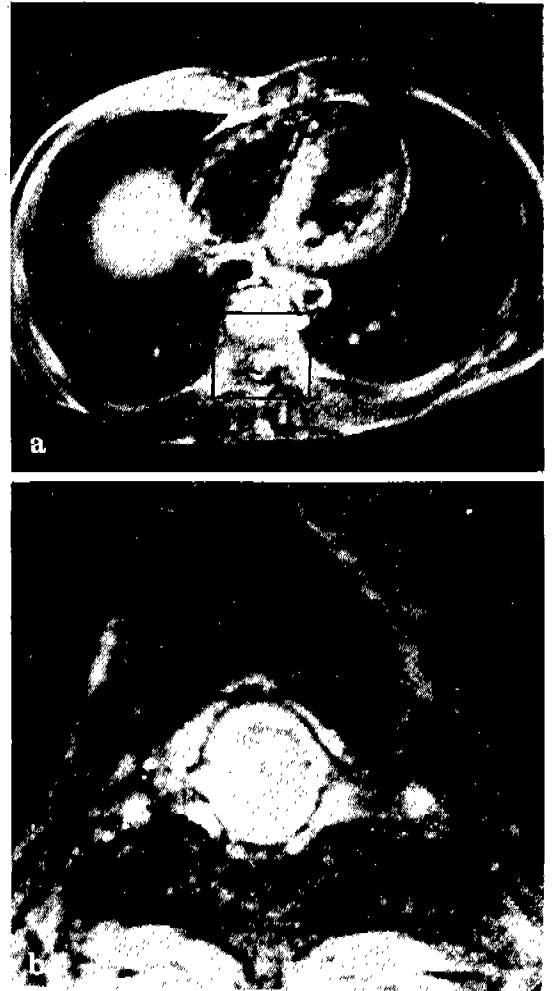


Fig. 5 Images of volunteer : (a) is a spin-echo image obtained by using conventional gradient coil and rf coil and (b) is a high-resolution ($200\mu\text{m}$) spinal cord image obtained by using SGC+surface rf coil set and conventional gradient-echo sequence with $T_R/T_E=800/9\text{ms}$.

mances by performing volunteer's high-resolution imaging. The new SGC is suitable for the high-resolution 3-D imaging since it provides good linearity and strong gradients by using conventional gradient coil driver. The new SGC expanded linear imaging region more than twice wider, removed the field offset and torque, and provided easy construction and easy combination with surface rf coil thereby developing a complete surface imaging probe. The combination of the SGC and the surface rf coil provides strong three orthogonal gradients, high sensitivity, localizing property, and the large accessible space of the objects to be imaged, which satisfy the essential requirements of *in vivo* high-resolution imaging of human body. The field gradients of the new SGC with the combined surface rf coil offers automatic localization. Accordingly one can obtain the high-resolution image of large object such as human body without complex localization. By adopting the SGC set to the conventional MRI system as we examined all the imaging experiments with KAIST 2.0T whole-body system, various high-resolution imaging will be possible by using convenient imaging sequences since the coil provides strong gradients by using the existion imaging system, thereby widening application area of MRI. For ultra-high resolution or microscopic imaging, size of the SGC can be scaled-down to obtain stronger and faster gradients while maintaining its flat structure and various merits.

REFERENCES

- 1) L. P. Clarke, H. N. Schnitzlein, F. R. Murtagh, and M. L. Silbiger, *Magn. Reson. Imag.* **4**, 515-523(1986).
- 2) K. P. Schellhas, *Magn. Reson. Imag.* **4**, 495-515(1989).
- 3) V. M. Rao, A. Babaria, A. Manoharan, S. Mandel, N. Gottehrer, H. Wank, and S. Grosse, *Magn. Reson. Imag.* **8**, 231-235 (1988).
- 4) D. L. Burk, Jr., M. K. Dalinka, E. Kanal, and J. A. Brunberg, "Magnetic Resonance Annual 1988", (ed. by H. Y. Kressel), p. 1, Raven Press, New York. 1988.
- 5) Z. H. Cho, C. B. Ahn, S. C. Juh, H. K. Lee, R. E. Jacobs, S. Lee, J. H. Yi, and J. M. Jo, *Med. Phys.* **15**(6), 815(1988).
- 6) J. H. Yi and Z. H. Cho, "in Abstracts of SmRm 9th Annual Meeting", p. 201, 1990.
- 7) Z. H. Cho and J. H. Yi, *J. Magn. Reson* **94**, 471(1991).
- 8) L. Axel, *J. Comput. Assist. Tomogr.* **8**(3), 381(1984).
- 9) G. S. Beveridge and R. S. Schechter, "Optimization : Theory and Practice", pp. 396-406, McGraw-Hill, 1970.
- 10) J. L. Keuster and J. H. Mize, "Optimization Techniques with Fortran", McGraw-Hill, USA, 1973.
- 11) C. S. Beightler, D. T. Phillips, and D. J. Wilde, "Fundamentals of Optimization", Prentice-Hill, USA, 1979.